

QUANTUM CHAOS: LOCALIZATION VS. ERGODICITY

B.V. CHIRIKOV, F.M. IZRAILEV and D.L. SHEPELYANSKY

Institute of Nuclear Physics, 630090, Novosibirsk, USSR

Received 14 January 1988

Results of theoretical and numerical studies of the quantum chaos are presented, and our current understanding of this phenomenon is discussed. The main attention is focused on the localization and ergodicity in classically fully chaotic quantum models, and on the related statistical properties of energy spectra as well as of eigenfunctions.

1. Introduction

The quantum chaos, a mysterious counterpart of the classical dynamical chaos is one of the most intriguing problems in physics currently under extensive studies by many researchers throughout the world. Professor Joseph Ford first addressed this difficult and exciting issue at the 1977 Como conference on Stochastic Behaviour in Classical and Quantum Hamiltonian Systems, organized by himself and Giulio Casati [1]. It was the first attempt to bring together various scientists who at that time worked separately in essentially the same direction. Joe Ford has greatly contributed to this field not only by studying and solving many particular problems but also by giving very interesting and original thoughts to the philosophy of dynamical chaos, both classical and quantal [2]. The present paper is a fragment in our current understanding of the phenomenon of quantum chaos which is gradually emerging, particularly from numerous discussions, and disputes, with Joe Ford.

Our starting point is the dynamical chaos in classical mechanics, or in the classical limit of quantum mechanics, as we usually say. This phenomenon is well understood by now (see, e.g. refs. [3, 4]). We think of dynamical chaos as random motion (in the sense of Alekseev) of a purely

dynamical system without any random parameters or any noise. According to the Alekseev–Brudno theorem (see ref. [5]) the necessary and sufficient condition for such a chaos is exponential local instability of motion on a set of initial conditions of dimension greater than one (to exclude the case of an isolated unstable periodic trajectory). Besides, the motion must be bounded, at least in some dynamical variables. The instability rate is characterized by the metric entropy h of Kolmogorov and Sinai (whose notation should not be confused with Planck's constant \hbar). The random (chaotic) motion remains unpredictable after any number of preceding measurements with any finite accuracy, nor is it reproducible by any finite (cellular) automaton (in particular, by a digital computer).

The ultimate origin of dynamical chaos lies in the continuity of the phase space in classical mechanics which implies an infinite amount of information related to almost any exactly fixed dynamical trajectory. The mechanism of local instability “unfolds” this information in time, so that asymptotically as $t \rightarrow \infty$ the specific information per unit time approaches the limiting value $J(t)/|t| \rightarrow h$ [5]. The time interval t_p , on which a partial prediction is still possible (“temporal determinism”), depends on the observation accuracy ϵ , and it is determined by the randomness parame-

ter [6]:

$$R = \frac{h|t|}{|\ln \varepsilon|} \sim \frac{|t|}{t_p}. \quad (1.1)$$

For $|t| \leq t_p$ ($R \leq 1$) a statistical description is also possible if ε is small enough while for $R \gg 1$ it is the only possibility (“asymptotic randomness”). Notice that randomness of the motion alone does not determine its statistical properties, which may happen to be rather unusual (see, e.g., ref. [7]).

Turning now to the more profound quantum mechanics we, first, separate the problem into two unequal parts: (i) the proper quantum dynamics that is the time evolution, including stationary states, of the state vector $\Psi(t)$, and (ii) the measurement with its unavoidable statistical effect of the irreversible Ψ collapse which is a sort of inevitable noise. In accordance with our dynamical approach, we shall restrict ourselves to the first problem only, as the other researchers in this field also do. To be more accurate, we assume that there are two measurements only: the first (complete) one fixes the initial state of a system while the second records the result of its evolution. Notice that unlike in classical mechanics, any intermediate measurement would generally change the quantum motion considerably.

In what follows we will discuss only Hamiltonian (nondissipative) systems, considering them to be the more fundamental ones. Phenomenological friction is but a crude approximation of the molecular Hamiltonian chaos which is inevitably related to some noise according to the fluctuation–dissipation theorem.

Furthermore, we are most interested in conservative systems with the energy surfaces closed in phase space. In this case the principal peculiarity of quantum mechanics – the phase space discreteness – manifests itself in a most explicit way which implies, in turn, the discreteness of the energy (and frequency) spectrum. The latter is not only incompatible with dynamical chaos but, in classical mechanics, is characteristic of the opposite limiting case, the regular motion. However,

the fundamental correspondence principle requires some transition to chaos in the semiclassical region. How could it be possible? This question has been posed and answered in ref. [8] by means of introducing characteristic time scales of quantum evolution.

The shortest (logarithmic) scale t_E , which we will term Ehrenfest’s scale, is of the order

$$ht_E \sim \ln q, \quad (1.2)$$

where h is the metric entropy (see above), and $q \sim \hbar^{-1}$ is some characteristic quantum parameter – a quantum number, for example (see also section 3 below). Apparently, this time scale was first discovered in ref. [9] (see also refs. [10, 8]). It is explained by the fast spreading of a narrow wave packet because of the local instability of chaotic motion in the classical limit. According to Ehrenfest’s theorem, a narrow packet follows the classical trajectory, hence its motion, on scale t_E , is as random as in the classical limit. However, upon a complete quantum measurement the quantity ε in eq. (1.1) reaches its minimal value, $\sim 1/q$, hence $R \sim 1$, and the whole Ehrenfest scale falls into the domain of temporal determinism.

Even though Ehrenfest’s scale grows very slowly with q , it grows indefinitely as $q \rightarrow \infty$ ($\hbar \rightarrow 0$). It is sufficient to provide transition to the classical chaos. However, it turns out that there exists a much longer (power law) scale t_D of quantum dynamics which is obviously a more important one. It is given by

$$\ln(\omega t_D) \sim \ln q. \quad (1.3)$$

Here ω is a characteristic classical frequency. On this (longer) scale, some important features of the classical chaos still persist, such as diffusion and statistical relaxation. This “diffusion scale” has been discovered in numerical experiments [1], and was explained in ref. [8]. Just this scale is going to be considered below (sections 4 and 5).

As $t \rightarrow \infty$ ($t \gg t_D$) the quantum nature of the evolution becomes decisive at any $q \rightarrow \infty$, and dynamical chaos manifests itself in a peculiar statistics of energy levels as well as in the structure of eigenfunctions (sections 6 and 7).

2. An example of true quantum chaos

The principal result of recent extensive studies in quantum chaos was the conclusion on its absence as was first pointed out by Krylov [11] in the late forties. However, there are some special cases when the true dynamical chaos proves to be possible in quantum mechanics as well.

Consider a classical dynamical system on an N -dimensional torus with angle variables θ_i :

$$\dot{\theta}_i = g_i(\theta_k), \quad i, k = 1, \dots, N. \quad (2.1)$$

Here the functions g_i are of period 2π in all θ_k . The chaos is possible in such a system for $N \geq 3$ (see, e.g., ref. [3]). It means that the equations of motion linearized about some trajectory $\theta_k^0(t)$

$$\dot{\xi}_i = \xi_k \left. \frac{\partial g_i}{\partial \theta_k} \right|_{\theta_k = \theta_k^0(t)}, \quad (2.2)$$

where $\xi_i = \theta_i - \theta_i^0$, are exponentially unstable, that is

$$\xi_i \sim e^{\Lambda_m t}. \quad (2.3)$$

Here Λ_m is the maximal Lyapunov exponent of the linear system (2.2).

The dynamics of system (2.1) can be described, for any functions g_i , by the conserved Hamiltonian

$$H = n_k g_k(\theta_i), \quad (2.4)$$

which implies the equations for the conjugate

momenta (cf. eq. (2.2))

$$\dot{n}_i = -n_k \frac{\partial g_k}{\partial \theta_i}. \quad (2.5)$$

Then, in the case of time-reversible dynamics, for example, the momenta also grow exponentially (2.3).

Now, consider a quantum system with Hamiltonian operator [12]

$$\hat{H} = \frac{1}{2}(g_k \hat{n}_k + \hat{n}_k g_k), \quad \hat{n}_k = -i \frac{\partial}{\partial \theta_k}. \quad (2.6)$$

Schrödinger's equation implies

$$\frac{\partial \rho}{\partial t} + \frac{\partial}{\partial \theta_k} (\rho g_k) = 0, \quad (2.7)$$

where $\rho = \Psi \Psi^*$ is the probability density, which coincides with the continuity equation for the classical system (2.1). Hence, the quantum probability would evolve exactly in the same way as the classical one, including the case of chaotic motion [12].

This simple example clearly demonstrates how extraordinary chaotic quantum dynamics has to be. Besides unbounded motion in momenta the latter are to grow exponentially fast. This is because the fine-grained (exact) probability density does not become homogeneous in time, as the coarse-grained density does; on the contrary, the former becomes more and more "scarred" by the mechanism of local instability of trajectories. This implies a fast growth of wave numbers, and, in quantum mechanics, of momenta.

3. The quantum rotator model

For studying the dynamics of classically chaotic quantum systems we have chosen the model of a

quantum rotator specified by the Hamiltonian [1]

$$\hat{H} = \frac{\hat{n}^2}{2} + k \cos \theta \cdot \delta_T(t). \quad (3.1)$$

Here the momentum is $\hat{n} = -i\partial/\partial\theta$; θ is the conjugate phase; $V = k \cos \theta$ is the perturbation function; $\delta_T(t)$ is the delta-function of period T , and we have set $\hbar = 1$. The dynamics of the corresponding classical system is described by the standard map [13]

$$\bar{p} = p + K \sin \theta, \quad \bar{\theta} = \theta + \bar{p}, \quad (3.2)$$

where $p = Tn$, and $K = kT$. The classical limit here corresponds to $k \rightarrow \infty$, $T \rightarrow 0$ while $K = kT = \text{const}$.

The dynamics of the quantum model (3.1) is also specified by a unitary mapping

$$\bar{\Psi} = \exp\left(i\frac{T}{2}\frac{\partial^2}{\partial\theta^2}\right) \exp(-ik \cos \theta) \Psi \quad (3.3)$$

and, unlike the classical model, essentially depends on both parameters k and T . In this model the perturbation is periodic in time. We mention that many particular physical problems can be reduced to such a model (see, e.g., ef. [14]).

Studying a map (especially numerically) is much simpler than a continuous model. This was precisely the main reason to choose model (3.1) from the beginning.

As we shall see right now the potential richness of this ‘‘simple’’ model is still far from being exhausted (see also ref. [7]). Particularly, system (3.1) may be thought of as a model of conservative dynamics, too. Indeed, in the classical limit a two-dimensional map of type (3.2) is related to some conservative system of two degrees of freedom (see, e.g., ref. [3]). Thus, such a map describes the local dynamics on the energy surface. To some extent, this should be true for the quantum map (3.3) as well.

Moreover, the model (3.1) can be modified to represent the global dynamics of a conservative system [16]. To this end we ‘‘close up’’ the

momentum axis p of the classical model (3.2) over some period p_0 , so that the infinite phase cylinder of map (3.2) is converted into a finite torus. The map remains smooth if $p_0 = 2\pi m_0$, with m_0 an integer. Then the period in n is $N = 2\pi m_0/T$, which is also the full number of quantum states for model (3.1) on a torus. Hence the quantity $T/2\pi = m_0/N$ is bound to be rational. For infinite quantum map (3.3) on a cylinder this would imply a very peculiar dynamics, the so-called quantum resonance [1, 15]. In the theory of this quantum phenomenon [15] the quantum map (3.3) is represented by a finite-dimensional unitary matrix U_{mn} of some dimension N .

To apply this theory to the finite quantum model on a torus, we may simply pick out only the solutions $\Psi(n, \tau)$ that are periodic in n in the momentum representation, and understand them as a finite Fourier series:

$$\Psi(\theta, \tau) = \sum_{n=-N_1}^{N_1} \Psi(n, \tau) e^{in\theta}, \quad (3.4)$$

where $N = 2N_1 + 1$ is odd, and τ is the number of map iterations.

The corresponding unitary matrix is conveniently represented in the following symmetric form:

$$U_{mn} = G_{mm'} B_{m'n} G_{n'n}, \quad (3.5)$$

where the diagonal matrix

$$G_{ll'} = \delta_{ll'} \exp\left(\frac{iT}{4} l^2\right) \quad (3.6)$$

describes a free rotation over time $T/2$, while the matrix

$$B_{mn} = \frac{1}{N} \sum_{l=-N_1}^{N_1} \exp\left(-ik \cos \frac{2\pi}{N} l\right) \times \exp\left(-i\frac{2\pi}{N} l(m-n)\right). \quad (3.7)$$

represents the effect of the perturbation (a ‘‘kick’’). In the semi-classical limit, the additional condi-

tion $NT = 2\pi m_0 = \text{const}$ ($N \rightarrow \infty$) should be satisfied. “Energy” levels ω_q of this model are always within the interval $(0, 2\pi)$, and are related to the eigenvalues λ_q of the unitary matrix U_{mn} by the expression $\lambda = \exp(i\omega)$.

Similar models on a sphere, rather than on a torus, were also studied (see, e.g., ref. [17]).

The dynamics of the classical infinite model (3.2) is completely determined by a single parameter K . Depending on its value there are two different regimes of motion: (i) bounded ($|\Delta n| \leq \sqrt{k/T}$), and (ii) unbounded. The critical K value separating them is most likely to be $K_{\text{cr}} = 0.9716\dots \approx 1$ [18]. Notice that in both regimes regular and chaotic components of motion coexist, the measure of the former vanishing as K grows [13].

At $K > K_{\text{cr}}$ the motion in the connected chaotic component may be described as a diffusion in n with the rate

$$D = \frac{\langle (\Delta n)^2 \rangle}{\tau} = \frac{D_0(K)}{T^2}, \quad (3.8)$$

where $D_0(K)$ is the diffusion rate in p for the map (3.2); τ the number of iterations.

In the semiclassical region, the classical diffusion persists within the diffusion time scale which is of the order $\tau_D \sim D \sim k^2$ [8]. For $\tau \ll \tau_D$ the quantum dependence $D_q(K)$ mimics all the details of the classical diffusion [19] in accordance with the correspondence principle.

The quantum diffusion stops for $\tau \gg \tau_D$, and turns into a stationary oscillation which was observed up to $\tau = 5 \times 10^4$ [20]. This would imply a discrete quasienergy spectrum for model (3.1) [8]. Hence, the “quantum chaos” is not true chaos as in the classical limit. Notice that deviations from the latter already begin on a much shorter scale (1.2) where $q = k$. Particularly, the local instability of quantum motion disappears at $\tau \gtrsim \tau_E$ [21, 22] while residual correlations persist [21, 23] (see also ref. [4]).

A striking illustration of dynamical stability in quantum chaos is afforded by a numerical experi-

ment with time reversal [23]. From the Hamiltonian (3.1) it follows that upon reversal $t \rightarrow -t$ at any instant $t = (m + \frac{1}{2})T$, with integer m , the system comes back to the initial state. In the classical limit the chaos results in the practical irreversibility of motion due to computation errors. Indeed, even at the accuracy $\varepsilon \sim 10^{-12}$ the instability destroys reversibility in just a few iterations $\tau_R \sim |\ln \varepsilon|/h \sim 10$ where $h \approx \ln(K/2)$. In a quantum system the instability is absent, and the reversibility accuracy is comparable, in order of magnitude, with ε [23]. Comparison of the initial probability distribution $|\Psi(\theta)|^2$ with that at the reversal instant of time, $\tau = 150$, and that of return to the initial state, $\tau = 300$, is shown in fig. 1. The difference in $|\Psi|^2$ at $\tau = 0$, and $\tau = 300$ is $\sim 10^{-10}$.

At $\tau = 150$ the wave function $\Psi(\theta)$ is a set of most narrow peaks whose width $\Delta\theta$ is determined by the number of excited states: $\Delta\theta \sim 1/\Delta n$, where roughly $\Delta n \sim (D\tau_D)^{1/2}$. The splitting into peaks in the diffusion process is the quantum counterpart of classical “scarring” of the distribution function for a chaotic motion. However, unlike exponentially fast splitting in a classical system, the quantum process goes on much slower, as a power law only, and even completely stops, as does the diffusion, for $\tau \gg \tau_D$.

4. Quantum localization principle for chaos

Following ref. [8] we first consider qualitatively the mechanism of diffusion limitation in model (3.1) using simple physical arguments. According to the correspondence principle, the quantum motion in the semiclassical region must be close, in some sense, to the classical one. This is obviously true on the shortest time scale τ_E until a wave packet is spread. At $\tau > \tau_E$ the quantum dynamics differs, of course, from the classical one [4], yet the classical diffusion still persists as the numerical simulation testifies [1, 8, 23].

For a continuous quasienergy spectrum the diffusion might go unbounded. The important point

is that in case of a discrete spectrum, with mean level density ρ_0 , the diffusion can still go on during a finite time interval

$$\tau \sim \tau_D \sim \rho_0. \quad (4.1)$$

It is directly inferred from the uncertainty principle that for $\tau \ll \rho_0$ the system does not resolve (“does not feel”) the spectrum discreteness pro-

vided the transitions between unperturbed states are efficient enough, that is, the perturbation exceeds Shuryak’s quantum border of stability [29]. In model (3.1) the latter is at $k \sim 1$ [1, 8]. Estimate (4.1) gives the diffusion time scale τ_D for model (3.1). It is important that the density ρ_0 in eq. (4.1) is determined by those eigenfunctions only which are actually present in a given quantum state, their effective number being always finite.

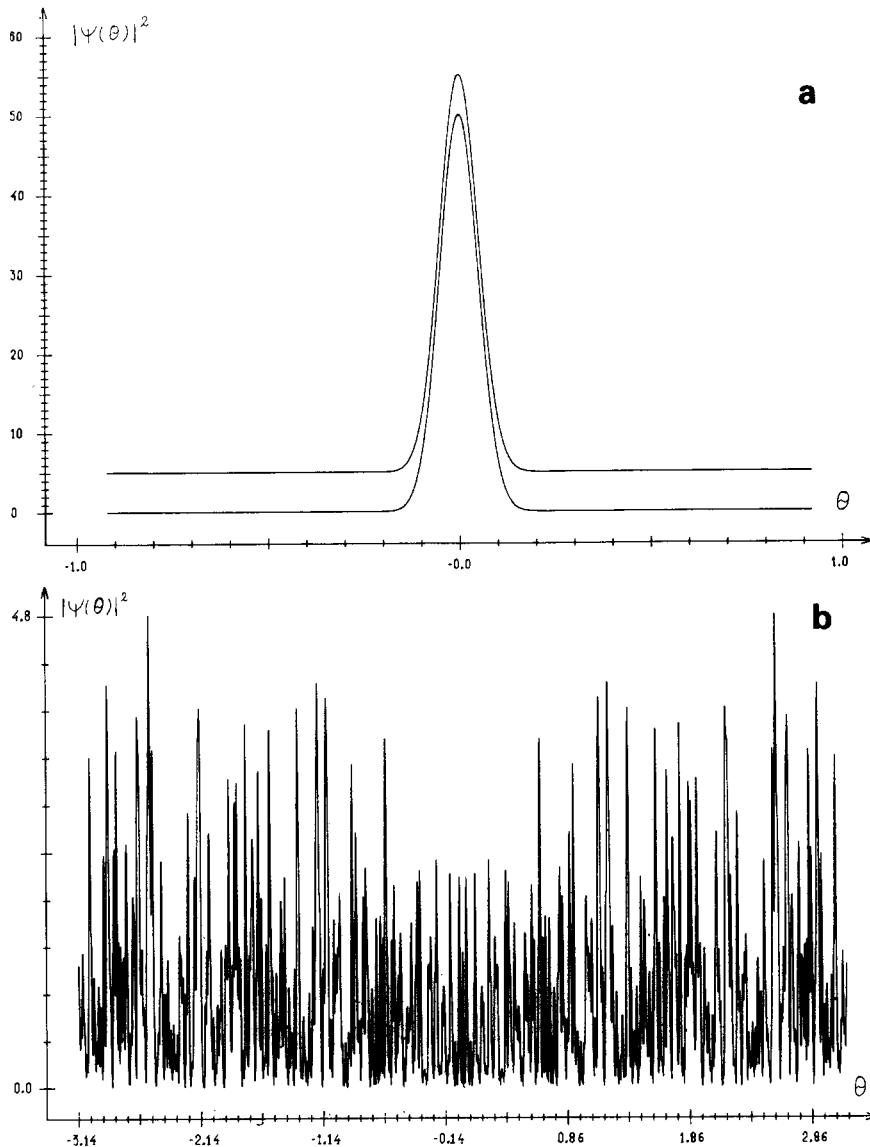


Fig. 1. Probability distribution in model (3.1) at different instances of time ($k = 20$; $K = 5$): (a) $\tau = 0$, initial Gaussian distribution (lower curve); $\tau = 300$, final distribution (upper curve, shifted upwards); (b) $\tau = 150$, time reversal.

Consider, first, the evolution of a single unperturbed state. The number of neighbouring unperturbed states excited due to diffusion during time τ_D would be $\Delta n \sim \sqrt{D\tau_D}$. It implies that the eigenfunctions are superpositions of many ($\sim \Delta n$) unperturbed states, and vice versa, any unperturbed state is represented by the same number of eigenfunctions. Assuming that quasienergies are homogeneously distributed within the interval $(0, 2\pi)$ we obtain $\rho_0 \sim \Delta n \sim \tau_D$, and

$$\tau_D \sim D \sim \Delta n \sim l, \quad (4.2)$$

where l is the effective number of unperturbed states finally excited after the diffusion is over. In other words, l is the localization length of eigenfunctions in n . Remarkably, estimate (4.2) relates essentially quantum characteristics, the diffusion scale τ_D and the localization length l , to the diffusion rate D in the classical limit.

The estimate (4.2) for τ_D apparently does not depend on the initial state apart from very unlikely states close to the eigenfunctions. As to the localization length l for the final state of a stationary distribution, eq. (4.2) holds only if the size of initial state $l_0 < l$. In the opposite case ($l_0 \geq l$) the size does not change at all.

5. Localization of quasienergy eigenfunctions, and of the stationary distribution

In ref. [24] a similarity was pointed out between the above-mentioned localization in momentum space (in n) and the well-known Anderson localization in a one-dimensional random potential (for the latter see, e.g., ref. [25]). The most important distinction between the two phenomena is that our model (3.1) has no random parameters. Also, the mechanism of localization in our model is, generally, completely different in various domains of the parameters. If $K \geq 1$ and $k \geq 1$ the localization is due to the hold-up of classical diffusion because of quantum interference effects. On the other hand, for $K < 1$ and $k \geq 1$ it is related to the

quantum tunnelling in a classically inaccessible region.

Borrowing an idea from solid state physics [25, 26], one can calculate the quantum localization length via Lyapunov exponents in an auxiliary classical Hamiltonian system [27]. An important advantage of this approach is in that one does not need to calculate the eigenfunctions, thus simplifying much of the numerical procedure. In the problem under consideration this method was also used in ref. [28].

For model (3.1) the equation for an eigenfunction φ_n with quasienergy ω can be written as [27]

$$\sum_r \varphi_{n+r} J_r \left(\frac{k}{2} \right) \sin \left(\frac{\omega}{2} - \frac{Tn^2}{4} - \frac{\pi r}{2} \right) = 0, \quad (5.1)$$

where J_r is the Bessel function. Because of sharp drop of J_r at $|r| > N \sim k/2$ one can leave a finite number $2N + 1 \sim k$ of terms in the sum. Then, the recursion, eq. (5.1), determines a $2N$ -dimensional dynamic system which turns out to be the Hamiltonian [27]. Hence, it has N positive (γ_i^+) and N negative (γ_i^-) Lyapunov exponents, and for each pair $\gamma_i^+ + \gamma_i^- = 0$. Asymptotically, the localization length l is determined by the minimal Lyapunov exponent $\gamma_1 = 1/l$, and the eigenfunctions behave like $\varphi_n \rightarrow \exp(-|n|/l)$ as $|n| \rightarrow \infty$. Hence, the quasienergy spectrum is purely discrete.

According to the theoretical estimate (4.2) the localization length is given by

$$l = \alpha D = \frac{D_0(K)}{2T^2}. \quad (5.2)$$

The numerical factor $\alpha = \frac{1}{2}$ has been obtained in ref. [27] by comparison with the exactly solvable Lloyd model. For this model the perturbation is $V(\theta) = 2 \arctg(E - 2k \cos \theta)$, and, in the quasilinear approximation, the diffusion rate is

$$D \approx D_{ql} = \frac{1}{2\pi} \int_0^{2\pi} \left(\frac{\partial V}{\partial \theta} \right)^2 d\theta. \quad (5.3)$$

Lyapunov exponents were computed using the standard techniques (see, e.g., ref. [3]) in the parameter range: $5 \leq k \leq 75$; $1.5 \leq K \leq 29$; $T \leq 1$ ($T/4\pi$ irrational), and D_0 varying by four orders of magnitude [27]. The mean value $\langle \alpha \rangle = 0.57 \pm 0.02$ (here and below statistical errors only are indicated). A slightly enhanced α value might be observed because the ratio $k/l \sim 0.1$ was not small enough.

Another way to check eq. (5.2) is by computation of the localization length for stationary distribution. Let the system be initially in state $n=0$, for example. The stationary distribution for $\tau \gg \tau_D$ is obtained by time averaging of probabilities $|\Psi(n, \tau)|^2$:

$$\bar{f}(n) \equiv \overline{|\Psi(n, \tau)|^2} = \sum_m |\varphi_m(0)\varphi_m(n)|^2, \quad (5.4)$$

where $\varphi_m(n)$ are the eigenfunctions. Notice that $\bar{f}(n)$ is the counterpart of the density–density correlation in the solid state problem [25]. Exponentially localized eigenfunctions may be represented as

$$|\varphi_m(n)| \sim \exp\left(-\frac{|n-m|}{l} + \xi_{nm}\right), \quad (5.5)$$

where ξ_{nm} describe fluctuations about average exponential dependence, and $\langle \xi_{nm} \rangle = 0$. Assuming that on the average

$$\langle |\varphi_m(n)|^2 \rangle \approx \frac{1}{l_s} \exp\left(-\frac{2|n-m|}{l_s}\right), \quad (5.6)$$

we obtain from eq. (5.4)

$$\bar{f}(n) \approx \frac{1 + 2|n|/l_s}{2l_s} \exp\left(-\frac{2|n|}{l_s}\right). \quad (5.7)$$

It may seem strange that the distribution localization length l_s is generally different from l for eigenfunctions. This is due to large fluctuations in ξ_{nm} . In the case of diffusively growing Gaussian

fluctuations,

$$\langle (\Delta \xi_{nm})^2 \rangle = D_\xi |\Delta n|,$$

we have, according to refs. [19, 27],

$$\begin{aligned} \frac{1}{l_s} &= \frac{1}{l} - \frac{D_\xi}{2}, & lD_\xi &\leq 1, \\ \frac{1}{l_s} &= \frac{1}{2l^2 D_\xi}, & lD_\xi &\geq 1, \end{aligned} \quad (5.8)$$

Again, a similar phenomenon is known in solid state physics [25].

An example of the stationary distribution is shown in fig. 2. The law (5.7) is verified approximately within a long range ($0 \leq x = 2|n|/l_s \leq 25$) over about 10 orders of magnitude in \bar{f}_N variations. A large-scale structure of $\bar{f}_N(x)$ is apparently related to fluctuations of ξ_{nm} .

Numerical simulation [19] in the parameter range $5 \leq k \leq 120$; $9 \leq l_s \leq 180$; $T \leq 1$ (D_0 variation comprises four orders of magnitude) results in $\langle \alpha_s \rangle = 1.04 \pm 0.03$ where $\alpha_s = l_s/D = l_s T^2/D_0$ (4.2), and l_s was numerically determined using eq. (5.7) (see fig. 2). Thus, $l_s \approx 2l$, and the diffusion rate in ξ_{nm} is

$$D_\xi \approx \frac{1}{l} \approx \frac{2}{D}. \quad (5.9)$$

Direct computation of D_ξ from the fluctuations of Lyapunov exponents gives $\langle lD_\xi \rangle \approx 1.14$ [27].

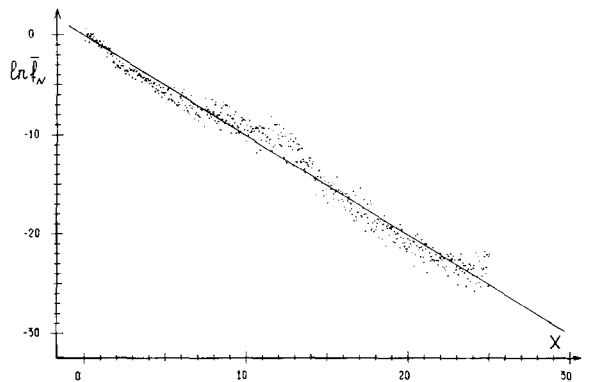


Fig. 2. Stationary distribution for $k=10$; $T=0.5$; $K=5$. Straight line: $\bar{f}_N = e^{-x}$; $\bar{f}_N = 2l_s \bar{f}(n)/(1+x)$; $x = 2n/l_s$.

Above we considered the asymptotic behaviour of eigenfunctions and of the stationary distribution at $n \gg l$. Those at $n \sim l$ are also of importance as they determine, for example, the mean energy of stationary oscillations, $E_s = \langle n^2 \rangle / 2$. If eq. (5.7) holds, then $\langle n^2 \rangle = l_s^2$, and $E_s = D^2 / 2$. This is also in a good agreement with our numerical data: $\langle 2E_s / D^2 \rangle = 0.92 \pm 0.04$.

6. Energy level statistics

Asymptotically as $t \rightarrow \infty$, the time evolution of any bounded quantum system (at least, a conservative one) is almost periodic because of its discrete energy (and frequency) spectrum irrespective of the motion in classical limit. This is just the opposite to the classical chaos (hence, the term “quantum pseudochaos” [30]). Yet, “remnants” of classical chaos still persist in peculiar statistical properties of the quantum spectrum, which will be discussed in this section, and of chaotic eigenfunctions to be considered in the next section 7.

These statistical properties have been studied since long ago, that led to the development of the random matrix theory, a statistical theory closest to the quantum dynamics (see, e.g., refs. [31, 32]). Until recently, however, this theory had been understood as some general description of a typical “complex” quantum system with many degrees of freedom. A striking resemblance to the traditional philosophy in statistical mechanics! Apparently, the relation of the statistics of quantum spectra to the dynamical chaos in classical limit was first considered in refs. [33, 34]. Much later numerical experiments on simple quantum models of only two degrees of freedom demonstrated surprisingly good agreement with random matrix theory, indeed [35]. This important result for the energy level statistics of a conservative system has been extended in ref. [36] to the quasienergies of the time-dependent model (3.1).

Here we consider the finite model (3.5) of a conservative quantum system as explained in section 3 above. Random matrix theory, particularly,

predicts that the distribution of nearest energy level spacings has the Wigner–Dyson form [31, 32]

$$p(s) = A s^\beta e^{-Bs^2}, \tag{6.1}$$

where A, B are normalizing constants; s the spacing with $\langle s \rangle = 1$, and the parameter $\beta = 1, 2$ or 4 depends on the system’s symmetry (for a new recent discussion of this dependence see refs. [36, 37]). For our finite model, $\beta = 1$.

In fig. 3, two characteristic examples of numerical data for model (3.5)–(3.7) are shown. Because of the spatial parity conservation the eigenfunctions are either even or odd: $\Psi_\omega(n) = \pm \Psi_\omega(-n)$ where ω is an “energy” eigenvalue. Both sets of eigenvalues were processed separately, and the

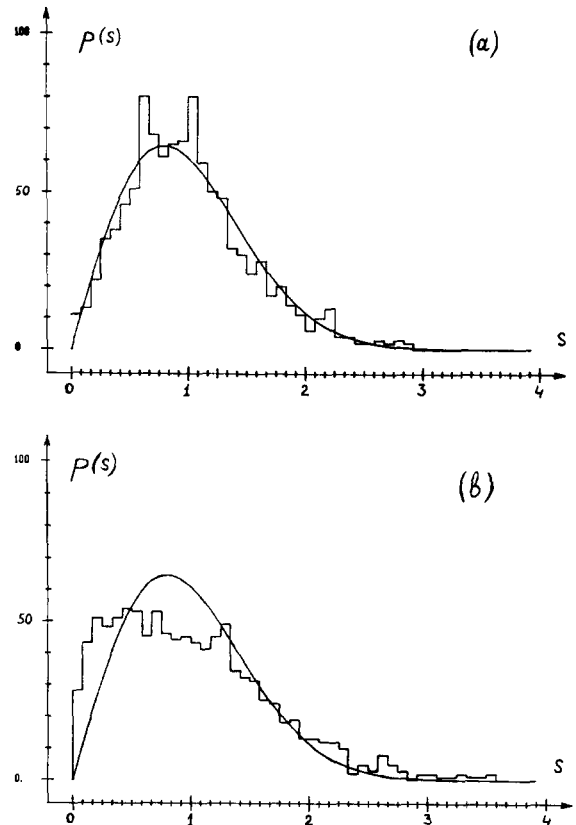


Fig. 3. Nearest energy level spacing distribution in model (3.5)–(3.7) for $T = 16\pi / (2N_1 + 1)$; $N_1 = 25$: (a) $k \approx 20$; $K \approx 20$; $l \approx 130$; $\Lambda \approx 5$; (b) $k \approx 5$; $K \approx 5$; $l \approx 6$; $\Lambda \approx 0.25$. Curves are Wigner–Dyson distribution (6.1), $\beta = 1$.

results were summed up. To further improve the statistics, 20 values of the parameter k were used with $\Delta k = 0.2$, the total number of energy levels amounting to $20 \times 51 = 1020$. The reduced spacing is $s = N_1 \Delta\omega / 2\pi$, where $\Delta\omega$ is the difference of nearest energy values, and $N_1 = (N - 1)/2 = 25$ the number of eigenfunctions with a given symmetry. The calculation accuracy in $\lambda = \exp(i\omega)$ was checked by the deviations $||\lambda| - 1| < 10^{-5}$.

For both cases in fig. 3, the classical motion is known to be fully chaotic [13] as $K = kT \gg 1$. Yet, the two distributions $p(s)$ reveal a striking difference. Our explanation is in that a new important parameter comes here into play, namely, the ratio $\Lambda = l/N_1$ of the localization length (section 5) to the dimensionality of eigenfunctions in Hilbert space that is the maximal number N_1 of (independent) unperturbed states coupled in an eigenfunction.

In one case (fig. 3(a)) $\Lambda \approx 5 \gg 1$, that is, the eigenfunctions are ergodic in the full unperturbed basis (see section 7 below). As a result there is a good agreement with random matrix theory (6.1), well confirmed by the χ^2 -criterion: $\chi^2(24) \approx 28.6$ which corresponds to a confidence level of 23 percent.

In the other case (fig. 3(b)) $\Lambda \approx 0.25 < 1$, which leads to an undisputable deviation $p(s)$ from eq. (6.1). Thus, random matrix theory is applicable to classically chaotic systems under the condition $\Lambda \gg 1$ only, and we call eq. (6.1) the “limiting statistics”. The new result for $\Lambda < 1$ we term “intermediate statistics” because there are good reasons to believe [36] that in the limit $\Lambda \rightarrow 0$ the distribution $p(s) \rightarrow \exp(-s)$ would approach the Poisson statistics of a completely integrable system in spite of chaos in the classical limit.

An important question arises: could the intermediate statistics be described by a one-parameter (Λ) family of distributions? A similar possibility was discussed by several authors and recently rejected in ref. [38] for a different kind of intermediate statistics due to the presence of regular motion in classical limit. In our case, however, we believe that it is true, indeed, and there exists a

universal distribution $p_u(s, \Lambda)$ connecting both limits, Poisson’s and Wigner–Dyson’s. Moreover, we conjecture that the localization parameter Λ must be related somehow to the inverse “temperature” β (6.1) in Dyson’s thermodynamical model of level repulsion [39]. This hypothesis is currently under study.

7. Chaotic structure of eigenfunctions

Even though random matrix theory considers statistical properties of both energy levels as well as eigenfunctions, until recently the former were studied almost exclusively. One reason was that the data on eigenfunctions are not directly available in laboratory experiments. However, this restriction does not take place in numerical simulation. The second, more profound, difficulty is that the eigenfunction structures, unlike the eigenvalues, are noninvariant under rotation of the basis. Particularly, there always exists a special basis – the eigenfunctions themselves – with trivial structure. In a sense, such bases are a priori very unlikely. In any event, it does not preclude the formulation and proof of a very important theorem [40] which states that in a classically ergodic system almost all eigenfunctions sufficiently far in the semiclassical region are also ergodic. In what follows we are going to make use of the unperturbed basis.

In the spirit of random matrix theory we define ergodicity by the condition $\langle |\Psi_m(n)|^2 \rangle = 1/N_1$, where $\Psi_m(n)$ is probability amplitude for the m th eigenfunction in the n th unperturbed state, and the normalization $\sum_{n=1}^{N_1} |\Psi_m(n)|^2 = 1$ is assumed. The averaging above is over either the same eigenfunction (in n), or different eigenfunctions (in m), or various matrices U_{mn} with different values of parameters, or any combination of the former.

The obvious condition for ergodicity is $\Lambda = l/N_1 \gg 1$. In the semiclassical region $l \sim k^2 \rightarrow \infty$, and $N_1 \sim m_0/T \sim m_0 k/K \rightarrow \infty$ so that $\Lambda \sim Kk/m_0 \rightarrow \infty$, which leads to ergodicity in accordance with Shnirelman’s theorem [40].

A more interesting and difficult question concerns the fluctuations of $\Psi_m(n)$. Gaussian fluctuations were conjectured in several papers (see, e.g., refs. [41]). Here we present our numerical results for model (3.5)–(3.7).

Because the matrix U_{mn} is unitary and symmetric, the real and imaginary parts of the eigenfunctions coincide. Hence, it is sufficient to study the eigenfunctions of the real part $\text{Re}(U_{mn})$. An example of a distribution of the values $\Psi \equiv \Psi_m(n)$ of different odd eigenfunctions $m = 1, \dots, N_1$ at different $n = 1, \dots, N_1$ for 20 different matrices U_{mn} is presented in fig. 4. Curve I shows the Gaussian distribution

$$w(\Psi) = \sqrt{\frac{N_1}{2\pi}} e^{-\Psi^2 N_1/2}, \quad (7.1)$$

assuming ergodicity $\langle \Psi^2 \rangle = 1/N_1$, and $\langle \Psi \rangle = 0$.

At first glance the agreement is fairly good. Yet, $\chi^2(38) = 98$, and the confidence level $< 10^{-6}(!)$. Hence, the fluctuations are close to Gaussian ones but certainly not exactly Gaussian.

Our explanation of this surprising disagreement relies upon the finite dimensionality, N_1 , of the eigenfunctions. As a result, Ψ fluctuations are strictly bounded by the condition $\Psi^2 \leq 1$, and an exact Gaussian distribution is impossible. Instead, we assume, following random matrix theory, the eigenfunctions to be invariant under any rotation

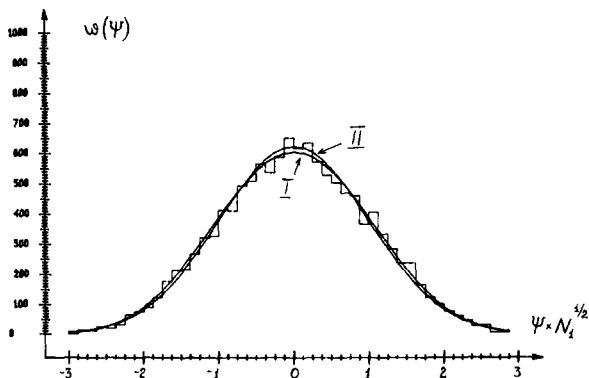


Fig. 4. Fluctuations of chaotic eigenfunctions for the parameters in fig. 3(a). Curve I is Gaussian distribution (7.1); curve II the distribution (7.2).

of the basis. Then (see, e.g., ref. [32])

$$w_{N_1}(\Psi) = \frac{\Gamma\left(\frac{N_1}{2}\right)}{\sqrt{\pi} \Gamma\left(\frac{N_1-1}{2}\right)} (1 - \Psi^2)^{(N_1-3)/2}, \quad (7.2)$$

where Γ is the gamma-function. This distribution is also shown in fig. 4 (curve II). The difference from a Gaussian distribution appears to be negligible. Yet, the χ^2 -criterion ($\chi^2(38) = 56$, 3 percent confidence level) clearly indicates a much better agreement of numerical data with eq. (7.2) which approaches the Gaussian distribution (7.1) in the limit $N_1 \rightarrow \infty$ only. This is again in agreement with random matrix theory provided the quantum system is ergodic ($\Lambda \gg 1$), and fully chaotic in the classical limit.

An additional check of eq. (7.2) is by calculation of the moments m_k of distribution (7.2) normalized to unity for Gaussian distribution. Comparison of analytical and numerical results,

$$m_2^{(a)} = 1,$$

$$m_2^{(n)} = 0.996 \pm 0.012,$$

$$m_4^{(a)} = \frac{1}{1 + \frac{2}{N_1}} = 0.926,$$

$$m_4^{(n)} = 0.888 \pm 0.030,$$

$$m_6^{(a)} = \frac{1}{\left(1 + \frac{2}{N_1}\right)\left(1 + \frac{4}{N_1}\right)} = 0.798,$$

$$m_6^{(n)} = 0.703 \pm 0.068,$$

also clearly shows deviations from a Gaussian distribution in agreement with random matrix theory. We emphasize again that unlike the later, our model has no random parameters.

During many years the present authors have greatly benefitted from permanent (though chaotic!) collaboration, discussions, and disputes with Professor Joseph Ford. May it last forever!

References

- [1] J. Ford et al., *Lecture Notes in Physics* 93 (1979) 334.
- [2] J. Ford, What is chaos, that we should be mindful of it? in: *Chaotic Dynamics and Fractals*, M.F. Barnsley and S.G. Demco, eds. (Academic Press, New York, 1985). J. Ford, Chaos: solving the unsolvable, predicting the unpredictable, in: *The New Physics*, S. Capelin and P. Davies, eds. (Cambridge Univ. Press, Cambridge, 1986). J. Ford, Quantum chaos: Is there any? in: *Directions in Chaos*, Hao Bai-Lin, ed. (World Scientific, Singapore, 1987).
- [3] A.J. Lichtenberg and M.A. Lieberman, *Regular and Stochastic Motion* (Springer, Berlin, 1983).
- [4] G.M. Zaslavsky, *Chaos in Dynamic Systems* (Harwood, New York, 1985).
- [5] V.M. Alekseev and M.V. Yakobson, *Phys. Rep.* 75 (1981) 287.
- [6] B.V. Chirikov, Intrinsic stochasticity, *Proc. Intern. Conf. on Plasma Physics, Lausanne* (1984), vol. 2, p. 761.
- [7] B.V. Chirikov and D.L. Shepelyansky, *Physica D* 13 (1984) 395.
- [8] B.V. Chirikov, F.M. Izrailev and D.L. Shepelyansky, *Sov. Sci. Rev. C2* (1981) 209.
- [9] G.P. Berman and G.M. Zaslavsky, *Physica A* 91 (1978) 450.
- [10] M. Berry et al., *Ann. Phys.* 122 (1979) 26.
- [11] N.S. Krylov, *Works on the Foundations of Statistical Physics* (Princeton Univ. Press, Princeton, NJ, 1979).
- [12] A.N. Gorban and V.A. Okhonin, Universality domain for the statistics of energy spectrum, preprint 29B, Inst. of Phys., Krasnoyarsk (1983).
- [13] B.V. Chirikov, *Phys. Rep.* 52 (1979) 263.
- [14] G. Casati, B.V. Chirikov and D.L. Shepelyansky, *Phys. Rev. Lett.* 53 (1984) 2525.
- [15] F.M. Izrailev and D.L. Shepelyansky, *Teor. Mat. Fiz.* 43 (1980) 417.
- [16] F.M. Izrailev, *Phys. Lett. A* 125 (1987) 250.
- [17] F. Haake, M. Kus and R. Scharf, *Z. Phys. B65* (1986) 381; *Lecture Notes in Physics* 282 (1987) 3.
- [18] J.M. Greene, *J. Math. Phys.* 201 (1979) 1183.
- [19] B.V. Chirikov and D.L. Shepelyansky, *Radiofizika* 29 (1986) 1041.
- [20] G. Casati, J. Ford, I. Guarneri and F. Vivaldi, *Phys. Rev. A* 34 (1986) 1413.
- [21] D.L. Shepelyansky, *Teor. Mat. Fiz.* 49 (1981) 117.
- [22] M. Toda and K. Ikeda, *Phys. Lett. A* 124 (1987) 165.
- [23] D.L. Shepelyansky, *Physica D* 8 (1983) 208.
- [24] S. Fishman, D.R. Grempel and R.E. Prange, *Phys. Rev. A* 29 (1984) 1639.
- [25] I.M. Lifshits, S.A. Gredeskul and L.A. Pastur, *Introduction into the Theory of Disordered Systems* (Nauka, Moscow, 1982) (in Russian).
- [26] J.L. Richard and J. Sarma, *J. Phys. C* 14 (1981) L127. A. MacKinnon and B. Kramer, *Phys. Rev. Lett.* 47 (1981) 1546.
- [27] D.L. Shepelyansky, *Phys. Rev. Lett.* 56 (1986) 677; *Physica D* 28 (1987) 103.
- [28] R. Blümel et al., *Lecture Notes in Physics* 263 (1986) 212.
- [29] E.V. Shuryak, *Zh. Eksp. Teor. Fiz.* 71 (1976) 2039.
- [30] B.V. Chirikov, *Found. Phys.* 16 (1986) 39.
- [31] C.E. Porter, ed., *Statistical Theory of Spectra: Fluctuations* (Academic Press, New York, 1965). M.L. Mehta, *Random Matrices* (Academic Press, New York, 1967).
- [32] T.A. Brody et al., *Rev. Mod. Phys.* 53 (1981) 385.
- [33] G.M. Zaslavsky and N.N. Filonenko, *Zh. Eksp. Teor. Fiz.* 65 (1973) 643.
- [34] I.C. Percival, *J. Phys. B* 6 (1973) L229; *Adv. Chem. Phys.* 36 (1977) 1.
- [35] O. Bohigas et al., *Phys. Rev. Lett.* 80 (1984) 157; *Lecture Notes in Physics* 209 (1984) 1.
- [36] F.M. Izrailev, Distribution of quasienergy level spacings for classically chaotic quantum systems, preprint INP 84-63, Novosibirsk (1984) (in Russian); *Phys. Rev. Lett.* 56 (1986) 541.
- [37] M. Robnik and M.V. Berry, *J. Phys. A* 19 (1986) 669.
- [38] M. Robnik, *J. Phys. A* 20 (1987) L495.
- [39] F.J. Dyson, *J. Math. Phys.* 3 (1962) 140, 157, 166.
- [40] A.I. Shnirelman, *Usp. Mat. Nauk* 29(6) (1974) 181.
- [41] M.V. Berry, *J. Phys. A* 10 (1977) 2083. M. Shapiro and G. Goelman, *Phys. Rev. Lett.* 53 (1984) 1714. E.J. Heller and R.L. Sunberg, in: *Chaotic Behaviour in Quantum Systems*, G. Casati, ed. (Plenum, New York, 1985), p. 255. B.V. Chirikov, *Phys. Lett. A* 108 (1985) 68.